Progress In Electromagnetics Research M, Vol. 112, 105–114, 2022

Hydrostatic Pressure Sensor Based on Defective One-Dimensional Photonic Crystal Containing Polymeric Materials

Sanjeev K. Srivastava*

Abstract—In this work, the design of a high sensitivity hydrostatic pressure sensor based on one-dimensional photonic crystal (1DPC) containing polymeric materials has been proposed and investigated, theoretically. The proposed structure consists of alternate layers of polystyrene (PS) and polymethyl metahacrylate (PMMA) with a defect of layer of PS, PMMA, and air, respectively, in the middle of the PC structure. The sensing principle is based on the shift in the peak of transmitted wavelength when the hydrostatic pressure is applied on 1DPC. In order to obtain the transmission spectrum of 1DPC structure transfer matrix method (TMM) has been used. From the analysis it is found that with the increase in hydrostatic pressure transmission (or resonance) peak shifts towards the lower wavelength side with respect to the center wavelength. The average sensitivity ($\frac{\Delta\lambda}{\Delta P}$) of the proposed sensor is found about 0.948 (nm/MPa) with polymer defect and 0.92 (nm/MPa) with air defect in the mid-IR frequency region, and the applied pressure range is 0 to 200 MPa.

1. INTRODUCTION

Photonic crystals (PCs) are artificial structure in which the refractive index of alternate layers varies periodically in a particular direction, and the thickness of periodic layers is comparable to the optical wavelength. PCs have generated much interest among the researchers and scientific communities due to their capability to control and manipulate the propagation of light wave [1–7]. Because of their unique properties to mold the flow of light, PCs have various potential applications in the field of photonics and optoelectronics [8–12].

Photonic crystal has two most important properties viz. existence of photonic band gaps (PBGs) and confinement or localization of photons [1, 2]. When electromagnetic wave falls on the PCs, the PCs prohibit the wave to pass through certain range of frequencies. The range of frequencies or wavelengths that do not allow the wave to pass through the PC is called photonic band gaps (PBGs) or forbidden bands. Moreover, photons can be localized or confined within the PBG by introducing the defect into the conventional PC. The defect inside the photonic crystal can be produced by breaking the spatial periodicity of the structure. The presence of defect layer creates a defect states inside the PBG. When the frequency (or wavelength) of incident photon is equal to defect state, the photon gets localized in the defect state, and resonant transmission mode is generated inside the band gap [13–20].

The wavelength or frequency of transmission mode can be tuned by two ways: (i) changing the concentrations or ingredients of constituents' materials and (ii) controlling the refractive indices of the materials. Refractive index of the defect layer can be controlled by changing the operating temperature, by applying an external electric and magnetic field, or by optical illuminations, and leads to various photonic devices [21–29].

Further, the refractive index and hence the defect mode can also be tuned by applying the hydrostatic pressure on the PC [30–37]. Xu et al. [30] and Yuan [31] studied 1D PC pressure sensor

Received 21 June 2022, Accepted 14 July 2022, Scheduled 28 July 2022
* Corresponding author: Sanjeev Kumar Srivastava (sanjeev17th@yahoo.co.in).
The author is with the Department of Physics, Amity Institute of Applied Sciences, Amity Uttar Pradesh, Noida 201301, India.

wherein they investigated the linear variation of transmitted light wavelength with the applied pressure. Ben-Ali et al. [32] investigated the effect of hydrostatic pressure and temperature on defective 1D PC for sensing application and reported very high sensitivity and quality factor of the proposed device.

The effect of applied pressure on the width of PBGs in 1D semiconductor-superconductor PCs has been investigated and studied by Herrera et al. [33]. Segovia-Chaves [34, 35] and his group reported the effect of hydrostatic pressure and temperature on the defect mode of 1D PC. The tunable mirrors and filters in 1D photonic crystals containing polymers with varying hydrostatic pressure have been investigated and studied by Jena et al. [37].

In this work, the design of a high sensitivity hydrostatic pressure sensor based on 1D-PC containing polymeric materials has been proposed and investigated, theoretically. The proposed structure consists of alternate layers of polystyrene (PS) and polymethyl metahacrylate (PMMA) with a defect of layer PS, PMMA, and air, respectively, in the middle of the PC structure. The reason to choose the polymeric materials is that they show elasto-optic effect, so their optical properties are very much tunable by applying pressure [37]. The pressure sensor proposed here is investigated in the mid-infrared region of the electromagnetic spectrum because the polymers PS and PMMA show excellent transparency in the frequency range 10–100 THz except some narrow absorption peaks in this range. However, these materials have no any absorption peaks in the spectral range lies between 60–65 THz, 4600 nm–5000 nm [38, 39].

2. THEORETICAL FORMULATION

To investigate the effect of hydrostatic pressure on the optical spectra of 1DPC, the proposed structures are modeled as [Air/$(AB)^N$/Air] and [Air/$(AB)^{N/2}D(AB)^{N/2}$/Air]. Figs. 1(a)–(b) show the schematic illustration of the proposed structure. In Figs. 1(a)–(b), A and B represent polystyrene (PS) and polymethyl methacrylate (PMMA) with refractive indices n_1, n_2 and thicknesses d_1, d_2, respectively. The period of lattice is $d = d_1 + d_2$, and N represents the total number of periodic layers. D represents

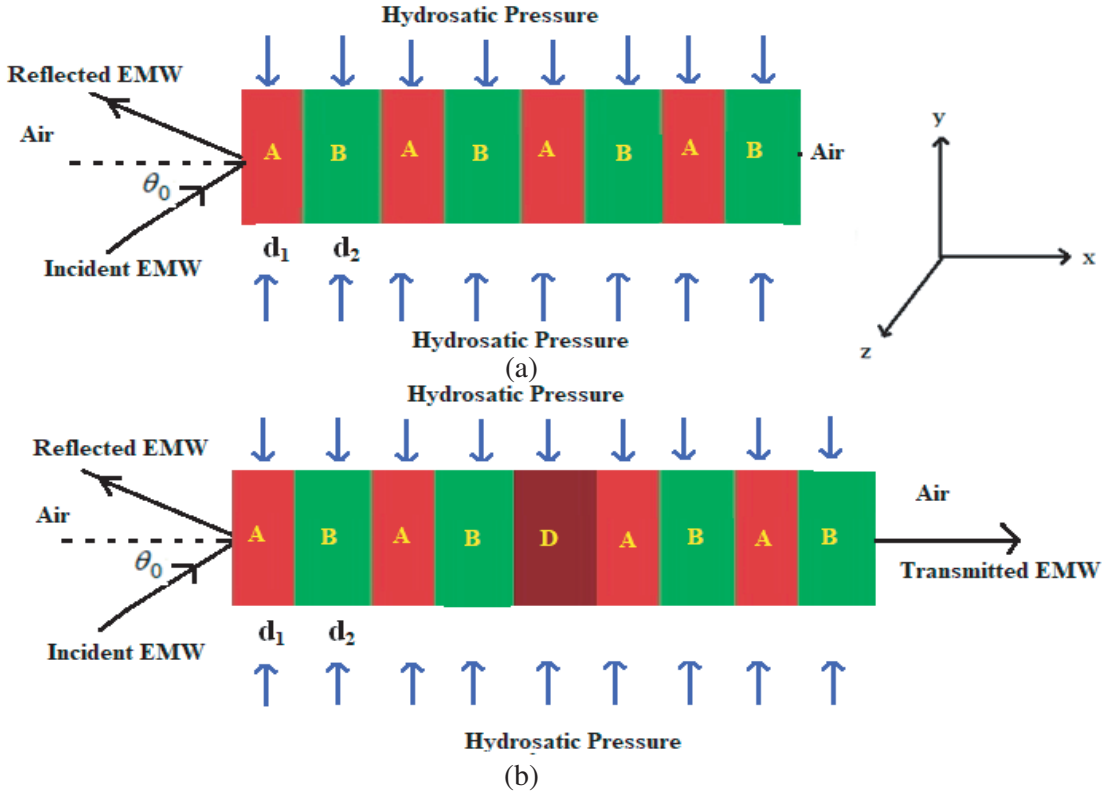

Figure 1. Schematic diagram of proposed 1DPC. (a) Normal PC. (b) Defect PC.

the defect layer with refractive index and thickness, n_3 and d_3, respectively.

In order to calculate the reflectance/transmittance spectra of proposed structure, we use transfer matrix method which is based on the Maxwell's equations and boundary conditions. Transfer matrix method (TMM) is very effective and simple technique used to study the transmission and reflection properties of finite photonic crystal.

Suppose light wave incident on 1D PC at an incident angle θ_0 along positive direction of x-axis from air (refractive index n_0). The electric and magnetic fields at the two interfaces of each are correlated by the transfer matrix method.

The characteristic matrix M_j for the jth layer in the PC for transverse electric (TE) and transverse magnetic (TM) waves can be given as [40, 41]

$$M_j = \begin{bmatrix} \cos\delta_j & \dfrac{1}{iq_j}\sin\delta_j \\ -iq_j\sin\delta_j & \cos\delta_j \end{bmatrix} \tag{1}$$

where $\delta_j = \frac{2\pi}{\lambda} n_j d_j \cos\theta_j$, $(j = A, B, D)$, θ_j is the ray angle inside the layer j of refractive index n_j, and λ is the wavelength of light in the incidence medium;

$$\begin{aligned} \cos\theta_j &= \sqrt{1 - \left(n_0^2 \sin^2\theta_0 / n_j^2\right)} \\ q_j &= n_j \cos\theta_j, \text{ for the TE wave and} \\ q_j &= \frac{\cos\theta_j}{n_j} \text{ for the TM wave.} \end{aligned}$$

The total characteristics matrix for the proposed PCs, having N period of system, is given by

$$M = \begin{bmatrix} M_{11} & M_{12} \\ M_{21} & M_{22} \end{bmatrix} = (M_A M_B)^N \tag{2}$$

For defective 1d-PC

$$\text{and} \quad M = (M_A M_B)^{N/2} M_D (M_A M_B)^{N/2} \tag{3}$$

where $M_A M_B$ and M_D are the characteristic matrices of layers A, B, and D, respectively. M_{11}, M_{12}, M_{21}, M_{22} are the elements of the total characteristic matrix of the N period multilayer structures.

The reflection and transmission coefficients for TE and TM waves are given by [41]

$$r = \frac{(M_{11} + q_t M_{12})\, q_0 - (M_{21} + q_t M_{22})}{(M_{11} + q_t M_{12}) q_0 + (M_{21} + q_t M_{22})} \tag{4}$$

$$t = \frac{2q_0}{(M_{11} + q_t M_{12}) q_0 + (M_{21} + q_t M_{22})} \tag{5}$$

The values of q_0 and q_t for TE and TM polarized waves are given as

$$\begin{aligned} q_0 &= n_0 \cos\theta_0; \quad q_t = n_t \cos\theta_t \quad \text{(For TE wave) and} \\ q_0 &= \cos\theta_0 / n_0 \quad q_t = \cos\theta_t / n_t \quad \text{(For TM wave)} \end{aligned}$$

Here, n_t is the refractive index of the substrate and θ_t the ray angle inside it. Finally, the reflectance and transmittance of the proposed PC structure can be determined by using the expression:

$$R = |r|^2 \tag{6a}$$

$$T = \frac{q_t}{q_0} |t|^2 \tag{6b}$$

The polymeric materials chosen for the study show good elasto-optic properties, and their refractive indices vary with applied hydrostatic pressure in the mid-infrared region of the electromagnetic spectrum. Further, the materials considered for the present study are assumed isotropic, elastic, and non-piezoelectric.

Under the applied hydrostatic pressure, the refractive index of polymeric material along the x-axis of the 1d-PC is given by [42, 43]

$$n(P) = \left[\varepsilon_0 - \frac{\varepsilon_0^2}{2}\left(\frac{p_{11}}{E}(\nu+1)P + \frac{p_{12}}{E}(3\nu+1)P\right)\right]^{1/2} \tag{7}$$

where ε_0 is the relative permittivity of the polymeric material without pressure; p_{11}, p_{12}, E, and v are the Pockels'coefficients, Young's modulus, and Possion's ratios of layers, respectively.

The sensitivity (S) is a significant parameter that determines the efficiency of the proposed pressure sensor. It is defined as the ratio of the change in the peak (resonant) wavelength to the change in the applied pressure. It is measured in nm/MPa

$$S = \frac{\Delta\lambda_{peak}}{\Delta P}$$

The other factor which determiners the efficacy of the device is the quality factor (Q). It is defined as the ratio of peak wavelength (λ_{peak}) to FWHM (Full Width at Half Maximum). The Q-factor basically expresses the sharpness of the transmission peak; its value should be as high as possible, for the better performance of the device.

$$Q = \frac{\lambda_{peak}}{FWHM}$$

3. RESULT AND DISCUSSIONS

In this section we compute the transmittance spectra of the proposed PC in the mid-IR region using MATHCAD software. The refractive indices of PS and PMMA layers have been calculated by using Eq. (7) for the parameters given in Table 1. The variation in refractive index of PS and PMMA materials with hydrostatic pressure is shown in Fig. 2. At $P = 0$ the refractive indices of PS and PMMA layers are 1.578 (n_1) and 1.484 (n_2), respectively. The thicknesses of the PS and PMMA layers

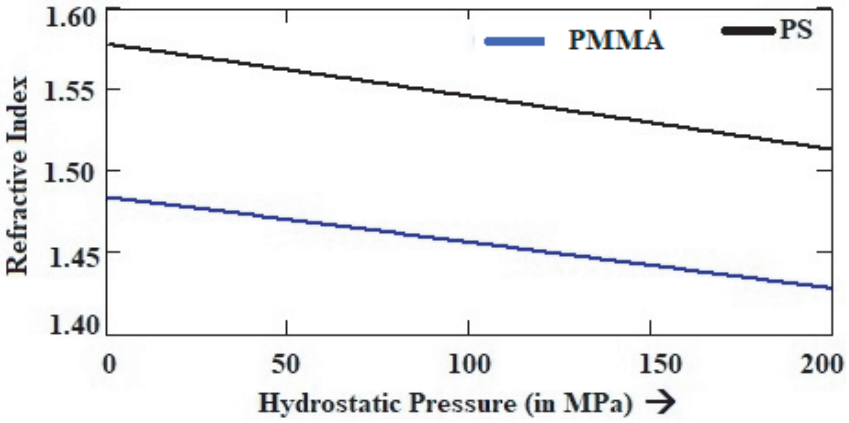

Figure 2. Variation of refractive index of PS and PMMA materials with hydrostatic pressure.

Table 1. Young's Modulus (E), Poisson's ratio (v) and Pockels coefficients for PS and PMMA material [42, 43].

Polymers	Young's Modulus E (in GPa)	Poisson's ratio (v)	Pockels coefficients	
			p_{11}	p_{12}
PS	3.3000	0.35	0.320	0.310
PMMA	3.0303	0.37	0.300	0.297

are chosen according to quarter wave stack condition $n_1 d_1 = n_2 d_2 = \frac{\lambda_0}{4}$ where $\lambda_0 (= 4800\,\text{nm})$ is the central wavelength, so $d_1(PS) = 760.4\,\text{nm}$ and $d_2(PMMA) = 808.6\,\text{nm}$. Further, the thickness of defect layer is also taken according to the quarter wave stack condition. Since the refractive index contrast between PS and PMMA is very low, in order to get maximum reflectivity in the desired spectral region, a large number of bilayers (N) are required, so $N = 70$. With these parameters the transmittance spectrum at normal incidence angle has been plotted for normal PC having the form [Air/(PS/PMMA)^N/Air]. Figs. 3(a)–(e) show the transmittance spectra of normal PC at different hydrostatic pressures P (in MPa) = 0, 50, 100, 150, and 200, respectively. From the transmittance spectra it can be observed that the width of reflection band (band gap) of PC decreases when the applied hydrostatic pressure is increased. At $P = 0$, reflection band lies in the range 4772 nm–4880 nm, having bandwidth 158 nm, but when hydrostatic pressure increases to 50 MPa, the width of reflection band gets reduced and becomes 153 nm (wavelength range 4677.5 nm–4830.5 nm). At $P = 100$, 150, and 200 MPa, the reflection band lies in the range 4632.9 nm–4778.0 nm (bandwidth 148.1 nm), 4588.3 nm–4731.6 nm (bandwidth 143.3 nm), and 4543.8 nm–4678.8 nm (bandwidth 135 nm), respectively. From the transmittance spectra it can be further noticed that edges (lower and higher) of the reflection band shift towards the lower side of the wavelength when the hydrostatic pressure increases. In other words, we can say that lower edge of the band moves away from the central wavelength ($\lambda_0 = 4800\,\text{nm}$), whereas higher edge of the band moves towards the central wavelength.

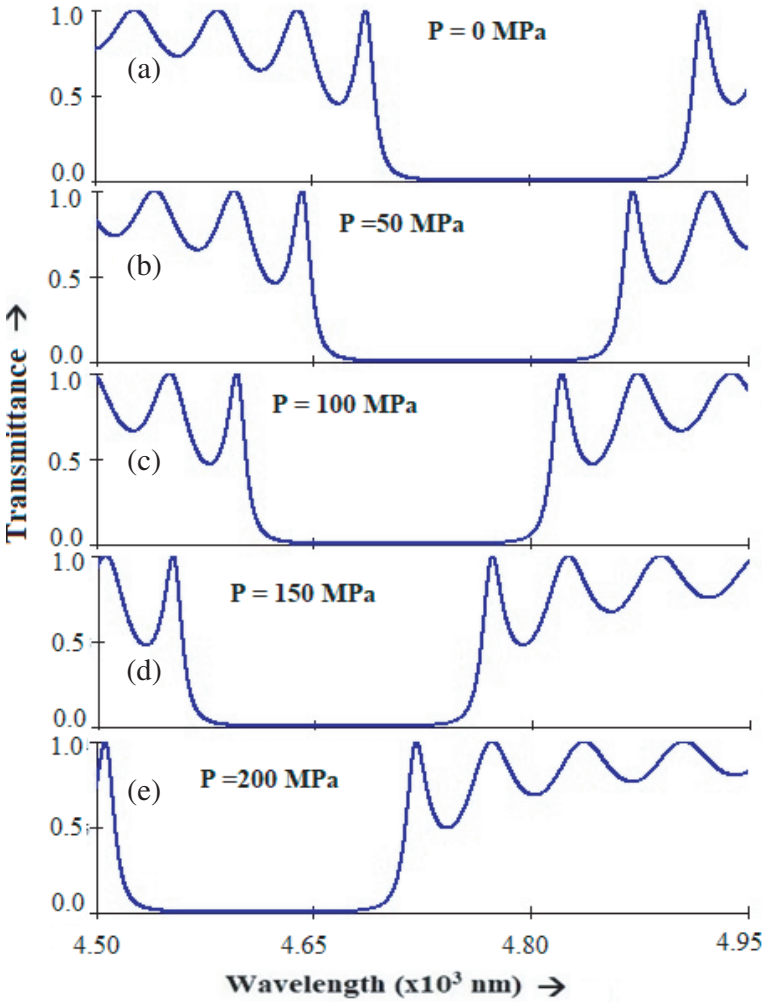

Figure 3. Transmittance spectra of 1DPC [Air/(PS/PMMA)^N/Air] for the parameters $\theta_0 = 0°$, $d_1 = 760.4\,\text{nm}$, $d_2 = 808.6\,\text{nm}$, $N = 70$ and at P (in MPa) = 0, 50, 100, 150 and 200 respectively.

The decrease in the width of reflection band of PC occurs due to decrease in refractive index contrast of the constituent materials (PS and PMMA) which arises by increasing the hydrostatic pressure.

But when we introduce the defect of PS, PMMA, and air respectively by breaking the periodicity of the normal PC then in the reflection band a transmission mode of wavelength is obtained. The transmission peak occurs at different wavelengths for different layers and varies at different applied pressures. Figs. 4(a)–(e) represent the transmittance curve for defect PC having the form $[\text{Air}/(\text{PS}/\text{PMMA})^{N/2}\text{PS}(\text{PS}/\text{PMMA})^{N/2}/\text{Air}]$ at normal incidence for different hydrostatic pressure P (in MPa) = 0, 50, 100, 150, and 200, respectively. From these figures, it is observed that transmission mode shifts towards lower side of the central wavelength when the hydrostatics pressure increases. At $P = 0$, the transmission peak lies nearly at 4800 nm (4799.8 nm), but when $P = 50$ MPa, there is significant change in wavelength of transmission mode, and it gets shifted to 4752.7 nm. The wavelength of transmitted modes of PS defected PC at different hydrostatic pressures $P = 0$, 50, 100, 150, and 200 MPa can be seen in Table 2. The shift in transmission peak is due to the change in the refractive index of defect layer (PS material) which decreases with increase in applied hydrostatic pressure.

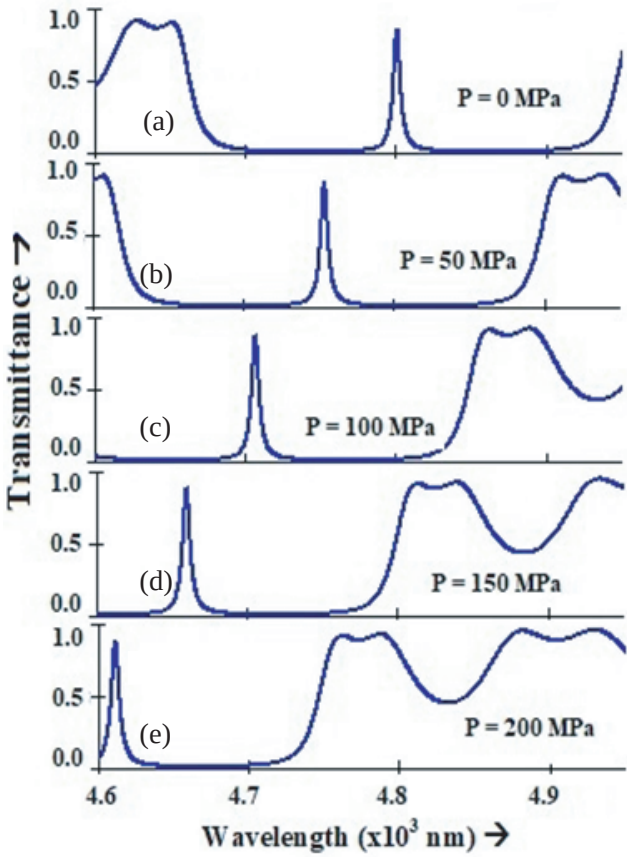

Figure 4. Transmittance spectra of 1DPC having form $[\text{Air}/(\text{PS}/\text{PMMA})^{N/2}\text{PMMA}/(\text{PS}/\text{PMMA})^{N/2}/\text{Air}]$ for $\theta_0 = 0°$, $d_1 = d_3 = 760.4$ nm, $d_2 = 808.6$ nm at pressure P (in MPa) = 0, 50, 100, 150 and 200, respectively.

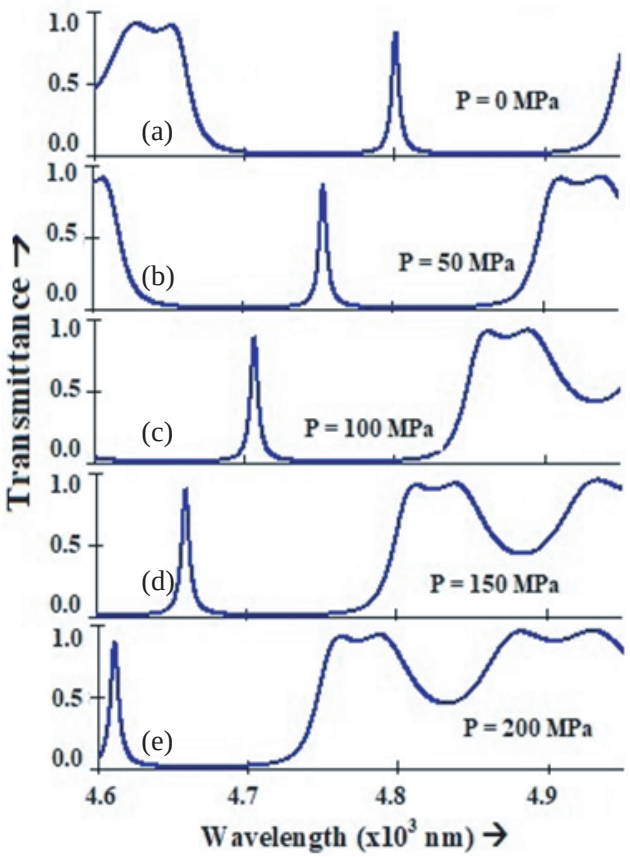

Figure 5. Transmittance spectra of 1DPC having form $[\text{Air}/(\text{PS}/\text{PMMA})^{N/2}\text{PMMA}/(\text{PS}/\text{PMMA})^{N/2}/\text{Air}]$ for $\theta_0 = 0°$, $d_1 = 760.4$ nm, $d_2 = d_3 = 808.6$ nm at pressure P (in MPa) = 0, 50, 100, 150 and 200, respectively.

The transmittance curves for $[\text{Air}/(\text{PS}/\text{PMMA})^{N/2}\text{PMMA}(\text{PS}/\text{PMMA})^{N/2}/\text{Air}]$ with varying hydrostatic pressure are depicted in the Figs. 5(a)–(e), and the wavelength of the transmitted peak is shown in Table 2. It can be seen that when PS defect layer is replaced by PMMA layer, the position of transmitted peak corresponding to the same applied pressure remains almost same as it occurs for PS defect PC. But the intensity of transmission peaks in PMMA defect PC is slightly higher than the

Table 2. The Wavelength of Transmitted Peaks (Modes) of 1DPC with PS defect, PMMA defect and Air defect at various hydrostatic pressures.

S.N.	Hydrostatic Pressure P (in MPa)	Wavelength of Transmission Peak (in nm)		
		PS Defect PC	PMMA Defect PC	Air Defect PC
1	0	4799.8	4799.8	4799.8
2	50	4752.7	4752.8	4754.1
3	100	4705.7	4705.9	4708.5
4	150	4658.7	4659.0	4662.9
5	200	4610.1	4610.6	4615.7

former one. The increase in intensity and slight shifts in the wavelength of transmission peak arise because PMMA layer has smaller value of refractive index than PS.

It can be noticed that the average change in the wavelength of transmitted mode, in both PCs, comes out to 47.4 nm for 50 MPa change in hydrostatic pressure. Thus, if we calculate the sensitivity of above sensor it is found to be 0.948 nm/MPa.

Further, from Figs. 4 and 5 it can be found that the quality factor $Q(=\frac{\lambda_{peak}}{FWHM})$ of the sensor decreases slightly by varying the hydrostatic pressure. The decrease in Q-factor is due to the shift in

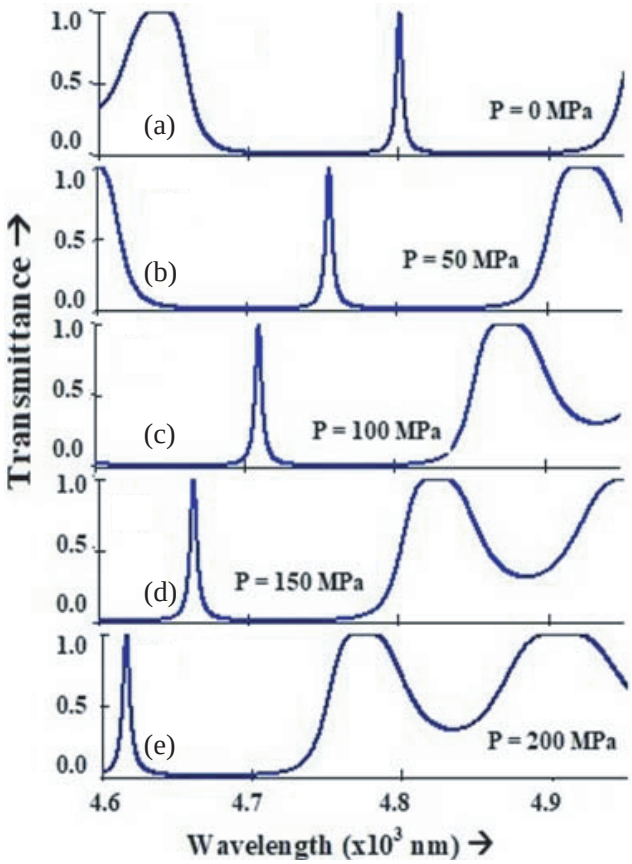

Figure 6. Transmittance spectra of 1DPC having form $[\text{Air}/(\text{PS}/\text{PMMA})^{N/2}\text{Air}/(\text{PS}/\text{PMMA})^{N/2}/\text{Air}]$ for $\theta_0 = 0°$, $d_1 = 760.4$ nm, $d_2 = 808.6$ nm, $d_3 = 1200$ nm at pressure P (in MPa) = 0, 50, 100, 150 and 200 respectively.

wavelength of transmission peak towards lower side of central wavelength, though FWHM is almost unaffected with the change in hydrostatic pressure.

Finally, the hydrostatic pressure sensing effect is studied on PC having air defect in the middle of the structure, i.e., [Air/(PS/PMMA)$^{N/2}$Air(PS/PMMA)$^{N/2}$/Air]. Figs. 6(a)–(e) illustrate the transmittance spectrum of air defect PC for the same parameters as taken above except the refractive index and thickness of air defect as $n_3 = 1.0$ (air) and thickness $d_3 = 1200\,\text{nm}$. Transmittance curves of air defect PC show similar trends in shifting of transmission peaks (modes) with varying hydrostatic pressure as seen in the polymeric defect PC. It is worth noting that using the air defect in place of PS and PMMA defect, the difference in wavelength of transmission peaks corresponding to the same variation in hydrostatic is comparatively smaller. At $P = 0$, transmitted peak lies at the same wavelength as in PS and PMMA defect PC, i.e., at 4799.8 nm. But when $P = 50\,\text{MPa}$ wavelength of transmitted peak shifts to 4754.1 nm, the change in wavelength of two consecutive transmitted peaks is 45.4 nm. The wavelengths of transmitted mode of air defect PC with different hydrostatic pressures are shown in Table 2. The average change in wavelength of transmitted peak is found as 46.02 nm with per 50 MPa change in hydrostatic pressure. Therefore, when the sensitivity of air defect PC is calculated, it comes out to 0.92 (nm/MPa), which shows a slightly less value than polymer defect PC structure. It can be further observed from Figs. 6(a)–(e) that the intensity of each transmitted mode is 100%, and the transmission peaks are sharper than the PS and PMMA defect PC. This causes a smaller value of FWHM of transmission curves and hence the increase in the quality factor of air defect PC structure.

4. CONCLUSIONS

In summary, the design of a high sensitivity hydrostatic pressure sensor based on 1DPC containing polymeric materials has been theoretically investigated and studied. The proposed structure consists of alternate layers of polystyrene (PS) and polymethyl metahacrylate (PMMA) with a defect of layer of PS, PMMA, and air, respectively, in the middle of the PC structure. The sensing principle is based on the shift in the peak of transmitted wavelength when the hydrostatic pressure is applied on 1DPC. Transfer matrix method has been employed to calculate the transmittance of 1DPC.

From the analysis of the proposed structure it has been observed that transmission (or resonance) peak shifts towards the lower wavelength side with respect to the center wavelength (reference wavelength) with the increase in hydrostatic pressure. The average sensitivity ($\frac{\Delta\lambda}{\Delta P}$) of the proposed sensor is found about 0.948 (nm/MPa) with polymer defect and 0.92 (nm/MPa) with air defect in the mid-IR frequency region, and applied pressure range is 0 to 200 MPa. Further, it is observed that the 1D-PC sensor having air defect exhibits high quality (Q) factor compared to the polymer defect in the proposed structure. This type of sensor can be used in long-distance pipeline strain monitoring and in environmental and biochemical sensing.

ACKNOWLEDGMENT

The author is thankful to Amity Institute of Applied Sciences, Amity University Uttar Pradesh, Noida, India, for providing the necessary facilities for this work.

REFERENCES

1. Yablonovitch, E., "Inhibited spontaneous emission in solid-state physics and electronics," *Phys. Rev. Lett.*, Vol. 58, 2059–2062, 1987.
2. John, S., "Strong localization of photons in certain disordered dielectric superlattices," *Phys. Rev. Lett.*, Vol. 58, 2486–2489, 1987.
3. Masaya, N., "Manipulating light with strongly modulated photonic crystals," *Rep. Prog. Phys.*, Vol. 73, 096501, 2010.
4. Jena, S., R. B. Tokas, P. Sarkar, J. S. Misal, S. MaidulHaque, K. D. Rao, S. Thakur, and N. K. Sahoo, "Omnidirectional photonic band gap in magnetron sputtered TiO_2/SiO_2 one dimensional photonic crystal," *Thin Solid Films*, Vol. 599, 138, 2016.

5. Zaghdoudi, J. and M. Kanzari, "One-dimensional photonic crystal filters using a gradient-index layer," *Optik*, Vol. 160, 189–196, 2018.
6. Srivastava, S. K. and A. Aghajamali, "Analysis of reflectance properties in 1D photonic crystal containing metamaterial and high-temperature superconductor," *J. Supcond. and Nov. Mag.*, Vol. 30, 343–351, 2017.
7. Srivastava, S. K., "Investigation of ultra-wide reflection bands in UV region by using one-dimensional multi quantum well photonic crystal," *Progress In Electromagnetic Research*, Vol. 38, 37–44, 2014.
8. Liu, G. Q., H. H. Hua, Y. B. Liao, Z. S. Wang, Y. Chen, and Z. M. Liu, "Synthesis and photonicband gap characterization of high quality photonic crystal heterostructures," *Optik*, Vol. 122, 9–13, 2011.
9. Aly, A. H. and Z. A. Zaky, "Ultra-sensitive photonic crystal cancer cells sensor with a high-quality factor," *Cryogenics*, Vol. 104, 102991, 2019.
10. Lee, M. and P. M. Fauchet, "Two-dimensional silicon photonic crystal based biosensing platform for protein detection," *Opt. Express*, Vol. 15, 4530–4535, 2007.
11. Rao, W., Y. Song, M. Liu, and C. Jin, "All-optical switch based on photonic crystal micro-cavity with multi-resonant modes," *Optik — Int. J. Light and Elec. Opt.*, Vol. 121, 1934–1936, 2010.
12. Abohassan, K. M., H. S. Ashour, and M. M. Abadla, "A 1D binary photonic crystal sensor for detecting fat concentrations in commercial milk," *RSC Advances*, Vol. 11, 12058–12065, 2021.
13. Smith, D., R. Dalichaouch, N. Kroll, S. Schultz, S. McCall, and P. Platzman, "Photonic band structure and defects in one and two dimensions," *JOSA B*, Vol. 10, 314–321, 1993.
14. Aly, A. H. and H. A. Elsayed, "Defect mode properties in a one-dimensional photonic crystal," *Physica B: Condensed Matter*, Vol. 407, 120–125, 2012.
15. Srivastava, S. K. and A. Aghajamali, "Narrow transmission mode in 1D symmetric defective photonic crystal containing metamaterial and high Tc superconductor," *Optica Applicata*, Vol. 49, 37–50, 2019.
16. Chang, T. W. and C. J. Wu, "Analysis of tuning in a photonic crystal multichannel filter containing coupled defects," *Optik — Int. J. Light and Elec. Opt.*, Vol. 124, 2028–2032, 2013.
17. Wu, C.-J. and Z. H. Wang, "Properties of defect modes in one-dimensional photonic crystal," *Progress In Electromagnetics Research*, Vol. 103, 169–184, 2010.
18. Ha, Y. K., Y. C. Yang, J. E. Kim, H. Y. Park, C. S. Kee, H. Lim, and J. C. Lee, "Tunable omnidirectional reflection bands and defect modes of a one-dimensional photonic band gap structure with liquid crystals," *Appl. Phys. Lett.*, Vol. 79, 15–17, 2001.
19. Lu, Y. H., M. D. Huang, S. Y. Park, P. J. Kim, T. U. Nahm, Y. P. Lee, and J. Y. Rhee, "Controllable switching behavior of defect modes in one-dimensional heterostructure photonic crystals," *J. Appl. Phys.*, Vol. 101, 036110, 2007.
20. Wang, Z. S., L. Wang, Y. G. Wu, and L. Y. Chen, "Multiple channeled phenomena in heterostructures with defects mode," *Appl. Phys. Lett.*, Vol. 84, 1629–1631, 2004.
21. Hung, H. C., C. J. Wu, and S. J. Chang, "Terahertz temperature dependent defect mode in a semiconductor dielectric photonic crystal," *J. Appl. Phys.*, Vol. 110, 093110-1–6, 2011.
22. Suthar, B. and A. Bhargava, "Temperature dependent tunable photonic channel filter," *IEEE Photon. Tech. Lett.*, Vol. 24, 338–340, 2012.
23. Chaves, F. S. and H. V. Posada, "Dependence of the defect mode on the temperature and angle of incidence in a one-dimensional photonic crystal," *Optik*, Vol. 163, 16–21, 2018.
24. Skoromets, V., H. Nmec, C. Kadlec, D. Fattakhova-Rohlfing, and P. Kužel, "Electric filed tunable defect mode in one-dimensional photonic crystal operating in the terahertz range," *Appl. Phys. Lett.*, Vol. 102, 241106-1–4, 2013.
25. Srivastava, S. K., "Electrically controlled reflection band and tunable defect modes in one-dimensional photonic crystal by using potassium titanyl phosphate (KTP) crystal," *J. Nano. Electron. Optoelctron*, Vol. 11, 284–289, 2016.
26. Tian, H. P. and J. Zi, "One-dimensional tunable photonic crystals by means of external magnetic fields," *Opt. Commun.*, Vol. 252, 321–328, 2005.

27. Pu, S., T. Geng, X. Chen, X. Zeng, M. Liu, and Z. Di, "Tuning the band gap of self-assembled superparamagnetic photonic crystals in colloidal magnetic fluids using external magnetic fields," *J. Magn. Magn. Mater.*, Vol. 320, 2345–2349, 2008.
28. Fan, C. Z., G. Wang, and J. P. Huang, "Magneto controllable photonic crystals based on colloidal ferrofluids," *J. Appl. Phys.*, Vol. 103, 094107, 2004.
29. Srivastava, S. K., "Magneto tunable defect modes in one-dimensional photonic crystal based on magnetic fluid film," *Springer Proc. Physics*, Vol. 256, 163–171, 2020.
30. Xu, X. Y., R. J. Zhang, and Y. L. Gong, "The principles of pressure sensor based on photonic crystal," *Acta Phys. Sin.*, Vol. 53, 724–727, 2004.
31. Yuan, Z. H., "Study on pressure sensor based on photonic crystal," *J. Transducer Technol.*, Vol. 24, 27–29, 2005.
32. Ben-Ali, Y., F. Z. Elamri, A. Ouariach, F. Falyouni, Z. Tahri, and D. Bria, "A high sensitivity hydrostatic pressure and temperature based on a defective 1D photonic crystal," *Journal of Electromagnetic Waves and Applications*, Vol. 34, No. 15, 2030–2050, 2020.
33. Herrera, A. Y., J. M. Calero, and N. P. Montenegro, "Pressure, temperature, and thickness dependence of transmittance in a 1D superconductor-semiconductor photonic crystal," *J. Appl. Phys.*, Vol. 123, 033101-1–5, 2018.
34. Segovia-Chaves, F. and H. Vinck-Posada, "The effect of the hydrostatic pressure and temperature on the defect mode in the band structure of one-dimensional photonic crystal," *Optik*, Vol. 156, 981–987, 2018.
35. Segovia-Chaves, F. and H. Vick-Posada, "The effect of hydrostatic pressure and temperature on the defect mode in a GaAs/Ga0.7Al0.3As one-dimensional photonic crystal," *Optik*, Vol. 159, 169–175, 2018.
36. Tao, S., D. Chen, J. Wang, J. Qiao, and Y. Duan, "A high sensitivity pressure sensor based on two-dimensional photonic crystal," *Photon. Sensors*, Vol. 6, 137–142, 2016.
37. Jena, S., R. Tokas, S. Thakur, and D. Udupa, "Tunable mirrors and filers in 1d photonic crystals containing polymers," *Physica E: Low-dimensional Systems and Nanostructures*, Vol. 114, 113627, 2019.
38. He, J., S. Chen, H. Huang, B. Chen, X. Xiao, J. Lin, and Q. Chen, "Novel anisotropic janus composite particles based on urushiol-erbium chelate polymer/polystyrene," *Soft Mater.*, Vol. 13, 237, 2015.
39. Duan, G., C. Zhang, A. Li, X. Yang, L. Lu, and X. Wang, "Preparation and characterizationof mesoporous zirconia made by using a poly (methyl methacrylate) template," *Nanoscale Res. Lett.*, Vol. 3, 118, 2008.
40. Yeh, P., *Optical Waves in Layered Media*, 118–125, John Wiley & Sons, New York, 1988.
41. Born, M. and E. Wolf, *Principles of Optics*, 4th Edition, 58–68, Pergamon, Oxford, 1970.
42. Sánchez, A. and S. Orozco, "Elasto-optical effect on the band structure of a one-dimensionalphotonic crystal under hydrostatic pressure," *J. Opt. Soc. Am. B*, Vol. 33, 1406, 2016.
43. Sánchez, A., A. Porta, and S. Orozco, "Photonic band-gap and defect modes of a one-dimensional photonic crystal under localized compression," *J. Appl. Phys.*, Vol. 121, 173101, 2017.